

Molecular conformations of dumbbell-shaped polymers in good solvent

Khristine Haydukivska,^{1,2} V. Blavatska,^{2,3} and Jarosław Paturej^{1,4,*}

¹*Institute of Physics, University of Silesia, 41-500 Chorzów, Poland*

²*Institute for Condensed Matter Physics of the National Academy of Sciences of Ukraine, 79011 Lviv, Ukraine*

³*Dioscuri Centre for Physics and Chemistry of Bacteria, Institute of Physical Chemistry, Polish Academy of Sciences, 01-224 Warsaw, Poland*

⁴*Leibniz-Institut für Polymerforschung Dresden e.V., 01069 Dresden, Germany*

(Dated: March 22, 2023)

We study conformational properties of diluted dumbbell polymers which consist of two rings that are attached to both ends of a linear spacer segment by using analytical methods of field theory and bead-spring coarse-grained molecular dynamics simulations. We investigate the influence of the relative length of the spacer segment to the length of side rings on the shape and the relative size of dumbbells as compared to linear polymers of equal mass. We find that dumbbells with short spacers are much more compact than linear polymers. Oppositely, we observe that the influence of side rings on the size of dumbbells becomes negligible with increasing length of a spacer. Consequently dumbbell molecules with long spacers become comparable in size with corresponding linear chains. Our analytical theory predicts quantitative cross-over between short- and long-spacer behavior and is confirmed by numerical simulations.

PACS numbers: 36.20.-r, 36.20.Ey, 64.60.ae

I. INTRODUCTION

In recent decades a lot of attention is directed to the research of polymers with complex architectures since they are characterised by unique physical properties. Particularly interesting are molecular architectures with no free ends with the simplest example being ring polymers, that have been thoroughly investigated[1–3]. Ring polymers are observed in nature in bacteria[4] and in some higher eukaryotes[5] which contain a circular DNA. Synthetic ring polymers are known to have a smaller size [6, 7] in solutions as well as no rubbery plateau in melts [8]. Mixtures of closed and opened chains demonstrate a number of interesting behaviours in melts[9]. However such mixtures are somewhat limited and it was suggested that tad-pole polymers with chains and rings chemically connected have a better threading topological constraints and provides a wider range of possible dynamic behaviour[10].

On another hand a wide range of research into the reology of pom-pom polymers was conducted in recent years[11–13]. With side arms influencing the reology of the melt[11].

In a recent study [14] a system of dumbbell polymers (see fig. 1) was investigated experimentally in both melt and solution. The presence of rings on both ends of the chain when they are threaded by the other dumbbell molecules is leading to the heavily constrained motion and thus a slow dynamic. On the other hand those same molecules in dilute solution have a similar behavior to that of the simple chains, in particular the similar values of viscosity were observed.

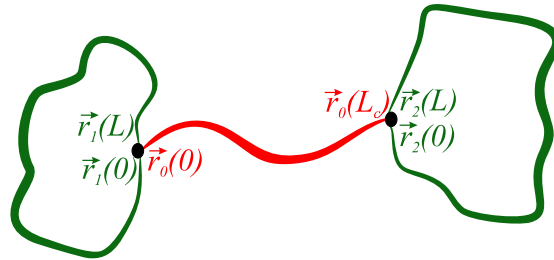


Figure 1: Schematic representation of dumb-bell polymer with side rings.

*E-mail: jaroslaw.paturej@us.edu.pl

Also polymer melts and dense solutions form the core of material applications, dilute solutions have their small roles as well, for example as a viscosity modifiers[1, 15, 16], as complex polymers are usually characterised by a lower intrinsic viscosity than their linear counterparts of the same mass. This is usually connected with the decrease in effective polymer size, with relation between intrinsic viscosity and effective size being described by the Flory-Fox equation [17, 18]. Another important goal that can be achieved by studying dilute solutions is that it allows to study the properties of individual molecules as in dilute solution the interactions between different macromolecules are neglectfully small[19].

The decrease in size for branched structures is measured by shrinking factor that is usually considered as a ratio between intrinsic viscosities of branched and linear macromolecules of the same molecular mass. In analytical descriptions a related ratio between the gyration radiuses is considered since the pioneering work of Zimm and Stockmayer[6]:

$$g_c = \frac{\langle R_g^2 \rangle}{\langle R_g^2 \rangle_{\text{linear}}} \quad (1)$$

Another example of the universal characteristics is asphericity ($\langle A_d \rangle$) [20]. The quantity A_d provides description of the shape of polymer configuration and distinguishes between spherical ($\langle A_d \rangle = 0$) and rod-like configurations ($\langle A_d \rangle = 1$). The asphericity is defined as:

$$\langle A_d \rangle = \frac{1}{d(d-1)} \left\langle \frac{\text{Tr} \hat{\mathbf{S}}^2}{(\text{Tr} \mathbf{S})^2} \right\rangle \quad (2)$$

where \mathbf{S} is the gyration tensor, $\hat{\mathbf{S}} = \mathbf{S} - \bar{\mu} \mathbf{I}$ with $\bar{\mu}$ being an average eigenvalue and \mathbf{I} a unity matrix. The quantities g_c and A_d are example of the so-called universal characteristics, that depends only on global properties of the system. In the case of polymers in dilute solutions such characteristic depends on the space dimension, quality of solvent, polymer branching and architecture but does not depend on the details of the monomer chemistry.

With a number of strategies for synthesis of complex polymers with rings developed [21] in recent decades including dumbbell[22, 23], sometimes called manacle-shape polymers[14], a theoretical consideration of universal characteristics may be of some academic interest.

In this work we consider the dumbbell polymers using both analytical and numerical approaches. We start with the short description of the methods used in this research in Section II that is followed by discussion of the results in Section III. We close this paper with concluding remarks in Section IV.

II. MODELS AND METHODS

A. Analytical model

An analytical description is conducted using field-theoretical continuous chain model [24]. In this model polymer chain is represented by a trajectory of length L parameterized by the radius vector $\vec{r}(s)$ where s varies from 0 to L . The Hamiltonian of the model is given as:

$$H = \frac{1}{2} \sum_{i=1}^F \int_0^{L_i} ds \left(\frac{d\vec{r}_i(s)}{ds} \right)^2 + \frac{u}{2} \sum_{i,j=1}^F \int_0^{L_i} ds' \int_0^{L_j} ds'' \delta(\vec{r}_i(s') - \vec{r}_j(s'')). \quad (3)$$

In the above equation F denotes functionality, i.e. a number of trajectories in the branched polymer architecture (for a dumbbell polymer it is $F = 3$) and u is a coupling constant that describes the strength of the excluded volume interactions. The polymer topology is introduced in the partition function of the system by fixing end(s) of trajectories:

$$Z_{L_c, L}^{\text{DB}} = \frac{1}{Z_0^{\text{DB}}} \int D\vec{r}(s) \times \delta(\vec{r}_1(0) - \vec{r}_0(0)) \delta(\vec{r}_2(0) - \vec{r}_0(L_c)) \times \delta(\vec{r}_1(0) - \vec{r}_1(L)) \delta(\vec{r}_2(0) - \vec{r}_2(L)) e^{-H}, \quad (4)$$

where $\delta(\vec{r}_1(0) - \vec{r}_0(0))$ and $\delta(\vec{r}_2(0) - \vec{r}_0(L_c))$ describe the connectivity of ring trajectories parameterized by vectors \vec{r}_1 and \vec{r}_2 to the ends of the linear trajectory \vec{r}_0 and the remaining two δ -functions impose geometrical constraints to

trajectories subjected them to form closed rings (see Fig. 1). Note that in our study we consider dumb-bell topologies with trajectories of different length. The linear backbone trajectory has the length L_c whereas the trajectory of side rings has the length L . We also point out that since both L and L_c in our analytical model are considered to be infinitely long the difference in length is introduced by considering the ratio $\lim_{L, L_c \rightarrow \infty} L_c/L = l$. We also note that in the continuous chain model the averaging over possible configurations that is performed in the partition function includes all types of knot conformations of the rings. Consequently these conformations are not distinguishable in our model. However since the rings are considered to be infinitely long [25] the knots are localized and do not influence neither scaling exponents nor the critical amplitudes [26–28].

In the continuous chain model the contribution from the excluded volume interactions is considered to be much smaller as compared to the Gaussian elasticity term. As a consequence all the observables are calculated as a perturbation series over the coupling constant u_0 [25]. In general the partition function has the following form:

$$Z(L, L_c) = Z_0 (1 - u_0 Z_1(l, d) + \dots) \quad (5)$$

where $u_0 = u(2\pi)^{-\frac{d}{2}} L^{2-\frac{d}{2}}$ is a dimensionless coupling constant. In the case of a dumbbell polymer $Z_0 = (2\pi L)^{-d}$. The second coefficient $Z_1(l, d)$ in the above equation represents the contribution from the excluded volume interactions and is calculated using the diagrammatic technique. The final expression for the coefficient $Z_1(l, d)$ as well as the details of calculations are provided in the Appendix (cf. Eq. (31)) All the observables can be written in a form of Eq. (5). In particular the radius of gyration is given as:

$$\langle R_g^2 \rangle = \langle R_g^2 \rangle_0 (1 - u_0 R_1(l, d) + \dots) \quad (6)$$

where $\langle R_g^2 \rangle_0$ denotes the contribution from the Gaussian conformation and the term R_1 is the first-order approximation of steric interactions. The explicit formula for term R_1 is provided in the Eq. (22) and the sketch of calculation of this term is given in the Appendix.

In the continuous chain model all observables are depend on the coupling constant u_0 that diverges as $L \rightarrow \infty$. In order to calculate finite physical value of the observable a renormalization has to be introduced such that $u_0^* \rightarrow u_R^*$ as the $L \rightarrow \infty$. The direct polymer renormalization approach for the model given by the Hamiltonian (cf. Eq. 3) leads to the following fixed points [25]:

$$\text{Gaussian : } u_R^* = 0, \quad \text{at } d \geq 4 \quad (7)$$

$$\text{EV : } u_R^* = \frac{\epsilon}{8}, \quad \text{at } d < 4. \quad (8)$$

where $\epsilon = 4 - d$ denotes the deviation from the upper critical dimension. A final result in this approach is usually given as a series in ϵ and an accurate quantitative result that can be compared with experimental data require at the very least the terms up to $\sim \epsilon^2$. However this is hard to achieve for a case of complex branched polymers. To overcome this problem we will use the method proposed by Douglas and Freed [7]. It starts by considering a generalized scaling form for the radius of gyration:

$$\langle R_g^2 \rangle = \langle R_g^2 \rangle_0 \left(\frac{2\pi N}{\Lambda} \right)^{2\nu(\eta)-1} f_p(\eta), \quad (9)$$

where N is the degree of polymerization, Λ is the coarse-graining length scale [29], and $f_p(\eta)$ is a function that controls the solvent quality with η being the crossover variable. It is equal 1 for $\eta = 0$ (Gaussian chain) and $1 + a$ for $\eta \rightarrow \infty$ which corresponds to the case of good solvent where a is topology-dependent parameter. At this point it is important to note that $\left(\frac{2\pi N}{\Lambda} \right)^{2\nu(\eta)-1}$ is the same for all molecular topologies which yields that the size ratio has the following general form:

$$g_x = \frac{\langle R_{g,1}^2 \rangle_0}{\langle R_{g,2}^2 \rangle_0} \frac{1 + a_1}{1 + a_2}. \quad (10)$$

This expression does not contain any approximations since the parameters a_1 and a_2 are the functions of ϵ . The approximation itself comes into play when the connection between a renormalization group approach and that of the two-parameter model for a $d = 3$ -dimensional space is made by expression:

$$a = \frac{3}{4} \frac{\epsilon}{8} R_1(l, d = 3) - \frac{1}{4} \quad (11)$$

where $R_1(l, d = 3)$ is the coefficient mentioned above but calculated for $d = 3$ which corresponds to two-parameter model calculation.

B. Molecular Dynamics Simulations

We consider a three-dimensional, bead-spring coarse-grained model [30] of a dumbbell polymer which is comprised of N spherical beads in each of two rings and N_c beads in the linear backbone. Each bead has the size σ_{LJ} and equal mass m . The nonbonded interactions between monomers are taken into account by means of the Weeks-Chandler-Anderson (WCA) interaction, i.e., the shifted and truncated repulsive branch of the Lennard-Jones potential given by

$$V^{\text{WCA}}(r) = 4\epsilon_{LJ} [(\sigma_{LJ}/r)^{12} - (\sigma_{LJ}/r)^6 + 1/4] \theta(2^{1/6}\sigma_{LJ} - r). \quad (12)$$

In the above equation r denotes a distance between the centers of spherical beads, while ϵ and σ_{LJ} are chosen as units of energy and length, respectively. In Eq. (12) is the Heaviside step function $\theta(x) = 0$ or 1 for $x < 0$ or $x \geq 0$. The bonds between subsequent beads are described by the Kremer-Grest potential [31] $V^{\text{KG}}(r) = V^{\text{FENE}}(r) + V^{\text{WCA}}(r)$, where the first term represents by the finitely-extensible nonlinear elastic (FENE) spring modelled by the following potential:

$$V^{\text{FENE}}(r) = -0.5kr_0^2 \ln[1 - (r/r_0)^2]. \quad (13)$$

with two constants $k = 30\epsilon/\sigma_{LJ}^2$ and $r_0 = 1.5\sigma_{LJ}$.

The simulations were conducted using the Large-scale Atomic/Molecular Massively Parallel Simulator (LAMMPS) [32], that solves the Newton's equations of motion using a velocity-Verlet algorithm. The temperature T was maintained by presence of the Langevin dumping term with the coefficient $\zeta = 0.5 m\tau^{-1}$, where $\tau = \sqrt{m\sigma_{LJ}^2/\epsilon}$ is the LJ time unit. The simulations were carried out in the cubic box with periodic boundary conditions in all three dimensions with equations of motion solved with the integration step $\Delta t = 0.005\tau$.

The initial conformations for the dumbbell polymers were generated using as a self-avoiding walk (SAW) technique generated by applying $20(2+l)N$ symmetry operations on the simple cubic lattice [33] (see detail on pivot algorithm). This approach allowed to start from a more compact conformations and save computation time since the method allows for more radical changes to the trajectories per step than the MD simulation. Note that the advantage of MD simulations is better sampling of conformations when calculating size ratios [34].

The simulations were run for up to 27 molecules in the simulation box, with the steric interactions between the molecules turned off to describe a dilute solution conditions. The data for the averaging of observables was accumulated for a time period of at least three relaxation times of the corresponding systems.

We considered dumbbell polymers with degree of polymerization of rings $N = 50, 100, 150, 200, 250$ and 300 beads and degree of polymerization of linear backbones of $N_c = N/4, N/2, N, 3N/2$ and $2N$. For each of value of N_c we calculated universal size ratios g in the asymptotic limit, i.e. by removing the finite size effects via a least-square fitting of the form: $g_c(N) = g + A/N^{0.53}$ with g and A being fitting constants. In the calculation of g factor (see Eq. (1)) we used the radius of gyration R_{linear}^2 of the corresponding linear chain of the same overall degree of polymerization as dumbbell molecule. The values R_{linear}^2 were obtained from a fitting function based on the simulations data in a range 100 to 600 beads where the expected scaling regime was observed. For the fitting the best known numeric values for the scaling exponent ν and the correction to scaling exponent Δ [35] were taken into account. This allowed us to utilize the most accurate values of R_{linear}^2 in the calculation of the size ratio g .

C. Wei's method

A complex macromolecule can be represented as a mathematical graph (network) where monomers are represented as vertices and chemical bonds between them as bonds of the graph. In this terms a degree of a node corresponds to the monomer functionality. The size and shape characteristics for any polymer network can be calculated using the Wei's method [36], which uses the Kirchhoff matrix and its eigenvalues.

A polymer that consists of N monomers is described by the Kirchhoff $N \times N$ matrix \mathbf{K} . All diagonal elements of this matrix K_{ii} are equal to degree of vertex i . The non diagonal elements K_{ij} are equal to either -1 or 0 for i and j being connected or not connected, correspondingly. A Kirchhoff matrix of size $N \times N$ has $N - 1$ non-zero eigenvalues $\lambda_2, \dots, \lambda_M$:

$$\mathbf{K}\mathbf{Q}_i = \lambda_i\mathbf{Q}_i, \quad i = 1 \dots M \quad (14)$$

and λ_1 is always 0. The size and shape characteristics within this model are given as functions of the above mentioned eigenvalues, thus the universal size ratio of Eq. (1) is defined as:

$$g = \frac{\sum_{j=2}^M 1/\lambda_j^{\text{network}}}{\sum_{j=2}^M 1/\lambda_j^{\text{linear}}}, \quad (15)$$

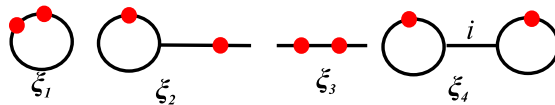


Figure 2: Schematic representation of diagrams for used in calculation of the radius of gyration in the Gaussian approximation. The polymer is depicted by solid lines and the bullets represent the so-called restriction points s_1 and s_2

where λ_j^{DB} and $\lambda_j^{\text{linear}}$ are the corresponding eigenvalues for the Kirchoff matrix describing architecture of either dumbbell or a linear chain.

The asphericity is given by the expression [36, 37]:

$$\langle A_d \rangle = \frac{d(d+2)}{2} \int_0^\infty dy \sum_{j=2}^M \frac{y^3}{(\lambda_j + y^2)^2} \left[\prod_{k=2}^M \frac{\lambda_k}{\lambda_k + y^2} \right]^{d/2}. \quad (16)$$

For a dumbbell architecture there are $N = (2+l)n + 2$ vertices with n being the number of vertices between the branching points (see Fig. 1) and every vertex having a degree $k > 1$.

III. RESULTS AND DISCUSSION

A. The radius of gyration of a dumbbell polymer and the universal size ratio

In the continuous chain model the radius of gyration of a dumbbell polymer is defined as:

$$\langle R_g^2 \rangle = \frac{1}{2((2+l)L)^2} \sum_{i,j=1}^3 \int_0^{L_i} \int_0^{L_j} \langle (\vec{r}_i(s_2) - \vec{r}_j(s_1))^2 \rangle ds_1 ds_2 \quad (17)$$

The actual calculation R_g^2 is performed by utilizing the following identity:

$$\begin{aligned} \langle (\vec{r}_i(s_2) - \vec{r}_j(s_1))^2 \rangle &= -2 \frac{d}{d|\vec{k}|^2} \xi(\vec{k})_{\vec{k}=0}, \\ \xi(\vec{k}) &\equiv \langle e^{-i\vec{k}(\vec{r}_i(s_2) - \vec{r}_j(s_1))} \rangle. \end{aligned} \quad (18)$$

where the contributions to $\xi(\vec{k})$ are calculated using the diagrammatic technique. The schematic representation of the diagrams in the Gaussian approximation are displayed in Fig. 2. The first two diagrams are counted twice and the later two only once. The final formula for the radius of gyration of a dumbbell polymer in the Gaussian approximation reads:

$$\langle R_g^2 \rangle_0 = \frac{dL}{6} (l+1)(l^2 + 5l + 3) \quad (19)$$

The corresponding universal size ratio (Eq. (1)) of a dumbbell polymer in the Gaussian approximation is given by the expression:

$$g_c = \frac{(l+1)(l^2 + 5l + 3)}{(l+2)^3} \quad (20)$$

Significantly larger set of diagrams need to be considered to estimate the radius of gyration of a dumbbell polymer with included excluded volume interactions. The calculation of R_g^2 in the first order of the perturbation theory, gives the following expression:

$$\langle R_g^2 \rangle = \frac{3L^3(l+1)(l^2 + 5l + 3)}{6} - u_0 R_1, \quad (21)$$

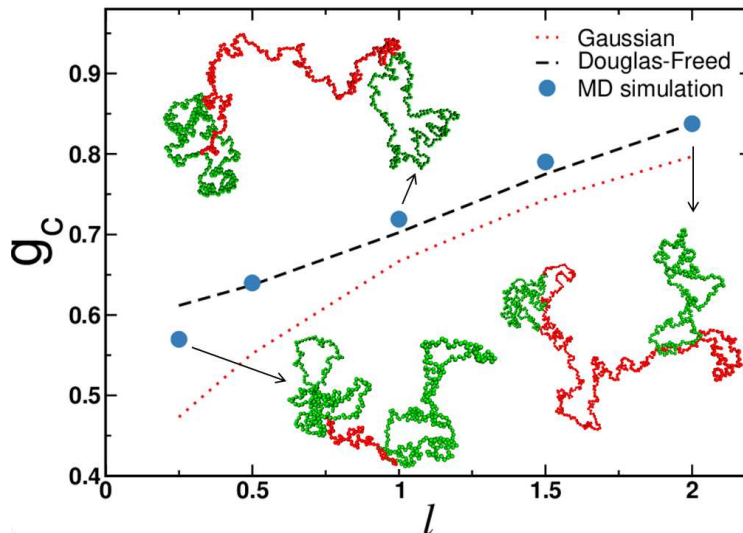


Figure 3: Relative size ratio g_c of dumbbell-shaped polymers with respect to the size of the corresponding linear polymer with the same overall degree of polymerization. Data plotted as a function of relative degree of polymerization l of linear chain monomers N_c to side ring monomers N . The lines represent theoretical prediction obtained for the Gaussian model (dotted line) and Douglas-Freed approximation (dashed line). The circles display the results of molecular dynamics simulations. The arrows indicate simulation snapshots for dumbbell polymers with given l .

where the term R_1 accounting for steric interactions is given by

$$R_1 = \frac{288l^2 - 964l - 85}{72} \arcsin\left((1+4l)^{-\frac{1}{2}}\right) - \frac{\pi(192l^2 - 332l + 47)}{72} - \frac{1072l^6 + 8308l^5 + 862l^4 + 42588l^3 + 36505l^2 + 7630l + 420}{630\sqrt{l}(1+4l)(2l+1)} - \frac{\arctan((2\sqrt{l})^{-1})}{3} - \frac{32l^4 - 1088l^3 - 2128l^2 - 1684l - 425}{144((2l+1)\sqrt{4l+2})} \left(\arctan\left(\frac{1+4l+\sqrt{4l+2}}{2\sqrt{l}}\right) - \arctan\left(\frac{1+4l-\sqrt{4l+2}}{2\sqrt{l}}\right) \right) \quad (22)$$

From a number of previous studies it is known that ϵ -expansion provides only a qualitative agreement with simulation and experimental data [7, 38–40]. From this reason in this work we do not provide the exact expression for g_c and limit our consideration to the Gaussian case (Eq. (20)) and the Douglas-Freed approximation. In the latter method the data was obtained numerically using the procedure described above.

In Fig. 3 we compare the results of our analytical calculations for the relative size g_c of ideal and real dumbbell polymers with respect to size of linear polymers and compare them with the results obtained from MD simulations. The data are plotted as a function of the relative degree of polymerization $l \equiv N_c/N$, i.e. the ratio between the number of monomers in a linear backbone to the number of monomers in a side ring. The red dotted line corresponds to the Gaussian approximation (i.e. ideal dumbbell polymer) and provides the lower boundary for g_c . The black dash-line represents the analytical results of the Douglas-Freed approximation for a real dumbbell polymer, i.e. with included excluded volume interactions. The MD results are plotted with blue circles. We observe very good agreement between simulation data with the analytical predictions. The data obtained from all the methods consistently show that the size ratio for dumbbell architectures with $l \leq 2$ is $g_c < 1$ indicating a smaller molecular size of these polymers as compared to linear counterparts of the same molecular mass. The ratio g_c increases with increasing l . For Gaussian dumbbell conformations in the limit of $l \rightarrow \infty$ it leads to the value of $g_c = 1$ whereas for real dumbbell conformations the limiting value for g_c obtained from the Douglas-Freed approximation is observed for $l \approx 5$ (data not shown). These results corroborate with the recent experimental study on dumbbell-shaped polymers carried out for large $l = 8$ where it was found that $g_c \approx 1$ [14]. We also point out that analytical calculations performed for H-polymers yield the value of $g_c = 1$ in the limit of $l \rightarrow \infty$, whereas for the case of $l = 5$ the corresponding ratio was found to be $g_c = 0.95$ [41].

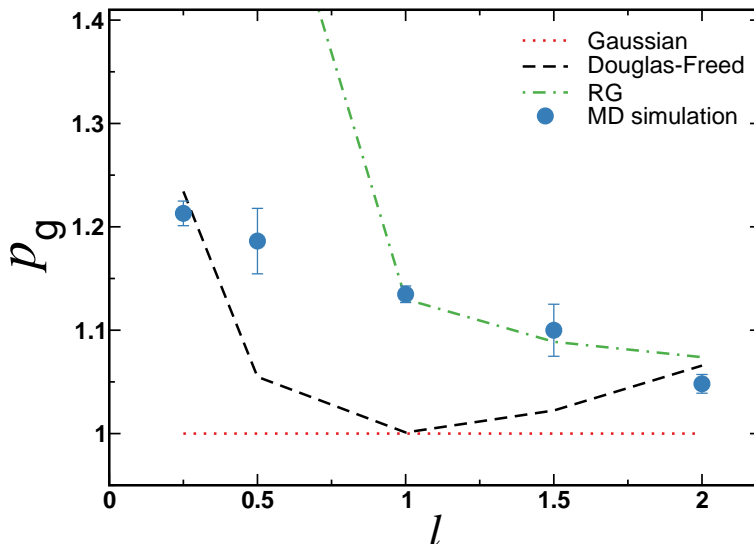


Figure 4: Relative size ratio p_g of the radius of gyration of dumbbell-shaped polymers to the radius of gyration of linear polymers plotted as a function of the relative degree of polymerization l . The lines represent theoretical predictions for the Gaussian conformations (dotted line), the Douglas-Freed approximation (dashed line) and the renormalization group calculations (dashed-dotted line). The symbols display the results of molecular dynamics simulations.

B. The radius of gyration radius of a dumbbell backbone and the corresponding size ratio

Another quantity that describes equilibrium conformation of a dumbbell molecule that is consider here is the gyration radius of dumbbell backbone defined as:

$$\langle r_g^2 \rangle_{\text{backbone}} = \frac{1}{2(lL)^2} \int_0^{L_c} \int_0^{L_c} \langle (\vec{r}_0(s_2) - \vec{r}_0(s_1))^2 \rangle \quad (23)$$

The strategy of calculation is similar to that of the full radius of gyration. The general expression for $\langle r_g^2 \rangle_{\text{backbone}}$ is:

$$\langle r_g^2 \rangle_{\text{backbone}} = \frac{dlL}{6} (1 - u_0 r_b(l, d) + \dots), \quad (24)$$

with $r_b(l, d)$ is the contribution from the excluded volume interactions. The explicit formula for $\langle r_g^2 \rangle_{\text{backbone}}$ is provided in the Appendix, cf. Eq. (38).

To describe the influence of dumbbell side rings on the stretching of its backbone we introduce the relative size with respect to the corresponding size of a linear chain:

$$p_g = \frac{\langle r_g^2 \rangle_{\text{backbone}}}{\langle R_g^2 \rangle_{\text{linear}}} \quad (25)$$

Unlike in the case of the universal size ratio g_c defined in Eq. (1), the quantity p_g does not depend on polymer topology for Gaussian conformations since it is simply equal to $p_g = 1$. In our analytical calculations of dumbbell conformations with steric interactions we accounted for topology-dependent contributions to p_g by considering the ϵ -expansion and Douglas-Freed approximation. In Fig. 4 we plot the values of p_g as a function of l obtained from theoretical methods (lines) and MD simulations (symbols). For $l \geq 1$, the data calculated from ϵ -expansion method (dashed-dotted line) is in good agreement with the simulation results. However for $l \leq 1$ these results significantly overestimate MD data. The reason for this is the presence of logarithmic terms ($\propto \ln(l)$) in the ϵ -expansion. Note that the results obtained from Douglas-Freed approximation (dashed line) do not provide a good agreement with the numerical results. This indicates necessity of the second order perturbation calculations to correctly capture stretching of the backbone.

C. Asphericity

In what follows we focus on the analysis of a shape of dumbbell polymers using asphericity factor. We emphasize that it is impossible to carry out path integration of the asphericity defined by Eq. (2) with the proper averaging.

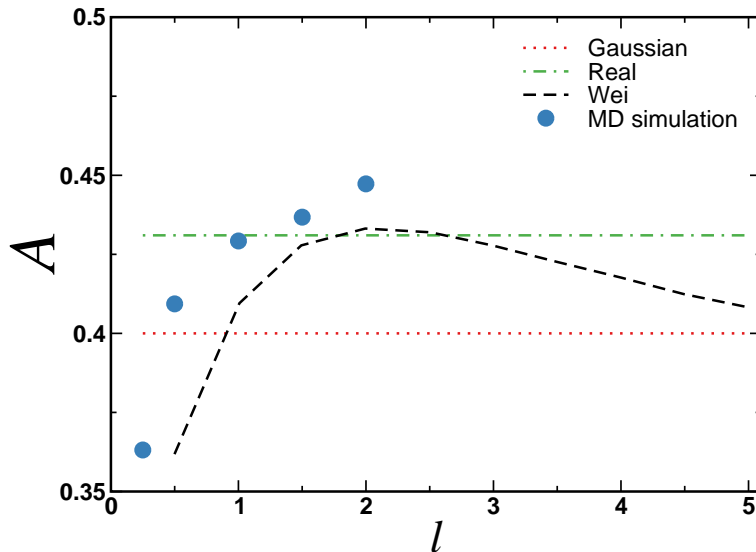


Figure 5: Asphericity A of dumbbell-shaped polymers plotted as a function of the relative degree of polymerization l . The lines represent predictions for Gaussian conformations (dotted line), real conformations (dashed-dotted line), i.e. with included steric interactions and the calculations using Wei’s methods. The symbols display the results of molecular dynamics simulations.

From this reason we limit our consideration to the Wei’s methods which provides good estimation of the asphericity for Gaussian conformations. Since in our calculations excluded volume interactions are introduced only as a small (perturbative) correction with respect to the Gaussian behavior, this approach is useful in predicting of a qualitative behavior of the molecule’s shape and includes molecular architecture of polymers. In Fig. 5 we display asphericity of dumbbell molecules calculated from the Wei’s method and plot it as a function of l (dashed line). We observe that for $l \gg 1$ asphericity decays towards the limiting value of $A = 0.4$ [42] known for Gaussian linear chain (dotted line). The similar trend is observed from our MD data (symbol) but in this case the limiting value of asphericity is $A = 0.431$ (dashed-dotted line) which is known from previous studies on a linear chain in good solvent [43].

IV. CONCLUSIONS

In this work we have studied the conformational properties of diluted dumbbell-shaped macromolecules consisting of two ring polymers connected to the ends of a linear spacer. For this purpose we used combination of analytical calculations using field-theoretical methods and molecular dynamic simulations. We have determined two relative size ratios g_c and p_g which are defined respectively as a ratio of the size R_g of a dumbbell and the size r_g of a linear spacer to the size R_{linear} of a linear chain of the same molecular weight. Our results indicate that conformations of dumbbells with short linear spacers are much more compact as compared to the linear polymer coils ($g_c < 0.65$). In this structural regime side rings have the major contribution to the global dumbbell conformation and cause stretching of the spacer segment ($p_g > 1$). Increasing the degree of polymerization of a spacer restores its conformational flexibility ($p_g \approx 1$) and gradually increases the size of a dumbbell molecule ($g_c \rightarrow 1$). Finally, for spacers that are much longer than side rings the size of a dumbbell matches the size of the corresponding linear chain ($g_c = 1$). Our numerical data for g_c are in a very good agreement with the analytical predictions. The theory correctly captures the cross-over of g_c with increasing length of a spacer. Our results also corroborate with the recent experiments that were carried out for dumbbells with long spacers [14] which reported $g_c \approx 1$.

Acknowledgments

J.P. and K.H. would like to acknowledge the support from the National Science Center, Poland (Grant No. 2018/30/E/ST3/00428) and the computational time at PL-Grid, Poland.

V. APPENDIX

Here we consider the details of the calculations of the contributions from the first order of perturbation theory to the partition function (Eq. 5) and the corresponding calculations of the radius of gyration of a dumbbell polymer (Eq. 6). In both cases a certain set of diagrams has to be considered. For the partition function the diagrams are the same as for the Gaussian approximation of the gyration radius (see Fig. 2). They only difference is that we include interaction points instead of restriction points. The corresponding expressions are given below:

$$Z_1 = u(2\pi)^{-\frac{d}{2}}(2\pi L)^{-d}L^{2-\frac{d}{2}}\frac{\Gamma\left(1-\frac{d}{2}\right)^2(2-d)}{2\Gamma(3-d)} \quad (26)$$

$$Z_2 = u(2\pi)^{-\frac{d}{2}}(2\pi L)^{-d}L^{2-\frac{d}{2}}\left(\frac{2^{d-2}\sqrt{\pi}\Gamma\left(2-\frac{d}{2}\right)}{(2-d)\Gamma\left(\frac{5}{2}-\frac{d}{2}\right)} - \frac{2^{d-1}(4l+1)^{1-\frac{d}{2}}}{d-2}\text{hypergeom}\left(\frac{1}{2}, \frac{d}{2}-1; \frac{3}{2}; \frac{1}{4l+1}\right)\right) \quad (27)$$

$$Z_3 = \frac{u(2\pi)^{-\frac{d}{2}}(2\pi L)^{-d}L_c^{2-\frac{d}{2}}}{\left(1-\frac{d}{2}\right)\left(2-\frac{d}{2}\right)} \quad (28)$$

$$Z_4 = u(2\pi)^{-\frac{d}{2}}(2\pi L)^{-d}L^{2-\frac{d}{2}}\int_{4l+1}^{4l+2}\frac{\left(\frac{x}{4}\right)^{-\frac{d}{2}}\text{hypergeom}\left(\frac{1}{2}, \frac{d}{2}; \frac{3}{2}; \frac{1}{x}\right)}{2\sqrt{2-x+4l}}dx \quad (29)$$

$$(30)$$

Here we would like to point out the complications encounter in calculations of the term Z_4 which contains an integral. However since this integral does not contain divergences in respect to $\epsilon = 4 - d$, we can perform the expansion of the integrand. As in one loop approximation we have to consider only the terms with pole and terms $\propto \epsilon^0$. Note that we effectively calculate the expression Z_4 only for the $d = 4$. Thus, the first order contribution into the partition function will read:

$$Z_1(l, d) = 2Z_1 + 2Z_2 + Z_3 + Z_4 \quad (31)$$

The calculation for the radius of gyration are conducted in the similar manner and are also complicated. Here, we have to calculate the set of diagrams displayed in Fig. 6. Here, diagrams 25, 26, 44 – 46 are reducible, as interaction points and restriction points do not share the same trajectory and thus the contributions are reduced to the product of the respective diagrams for the partition function and the Gaussian approximation for the radius of gyration. In general the calculation of the radius gyration is written as:

$$\begin{aligned} \langle R_g^2 \rangle &= Z^{-1}(\langle R_g^2 \rangle_0 - u(\text{Sum of diagrams})) = \langle R_g^2 \rangle_0 Z^{-1} \left(1 - u \frac{(\text{Sum of diagrams})}{\langle R_g^2 \rangle_0} \right) = \\ \langle R_g^2 \rangle_0 (1 + u Z_x) &\left(1 - u \frac{(\text{Sum of diagrams})}{\langle R_g^2 \rangle_0} \right) = \langle R_g^2 \rangle_0 \left(1 - u \left[\frac{(\text{Sum of diagrams})}{\langle R_g^2 \rangle_0} - Z_x \right] \right) \end{aligned} \quad (32)$$

Note that any contributions that appear in the product $Z_x \langle R_g^2 \rangle_0$ cancel out. These are the diagrams mentioned above and some parts of the remaining diagrams, that in the case of the radius of gyration are easily identifiable. As an example we consider diagrams 9 – 11:

$$\begin{aligned} &\int_0^S ds \int_0^L dz \int_s^L ds_2 \int_s^{s_2} ds_1 \left(s_2 - s_1 - \frac{(s_2 - s_1)^2}{s + z - \frac{s^2}{L}} \right) (s + z - \frac{s^2}{L})^{-\frac{d}{2}} + \\ &\int_0^S ds \int_0^L dz \int_s^L ds_2 \int_0^s ds_1 \left(s_2 - s_1 - \frac{(s - s_1)^2}{s + z - \frac{s^2}{L}} \right) (s + z - \frac{s^2}{L})^{-\frac{d}{2}} + \\ &\int_0^S ds \int_0^L dz \int_0^s ds_2 \int_0^{s_2} ds_1 (s_2 - s_1) (s + z - \frac{s^2}{L})^{-\frac{d}{2}} \end{aligned} \quad (33)$$

Since all three integrals contain the same factor $(s+z)^{-\frac{d}{2}}$ that does not depend on the restriction points this expression can be rewritten as:

$$\begin{aligned} &\int_0^S ds \int_0^L dz \left[\int_0^s ds_2 \int_0^{s_2} ds_1 \left(s_2 - s_1 - \frac{(s_2 - s_1)^2}{s + z - \frac{s^2}{L}} \right) + \right. \\ &\left. \int_s^L ds_2 \int_0^s ds_1 \left(s_2 - s_1 - \frac{(s - s_1)^2}{s + z - \frac{s^2}{L}} \right) + \int_s^L ds_2 \int_s^{s_2} ds_1 (s_2 - s_1) \right] (s + z - \frac{s^2}{L})^{-\frac{d}{2}} \end{aligned} \quad (34)$$

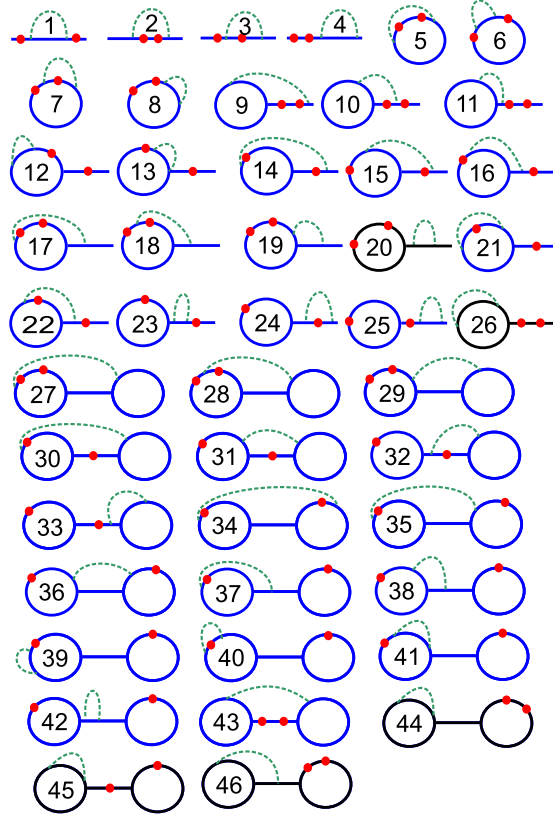


Figure 6: Schematic representation of diagrams utilized in calculation of the radius of gyration radius in one loop approximation. The polymer is depicted by solid lines and the bullets represent the so-called restriction points s_1 and s_2 . Dash-line represents the excluded volume interactions.

All the integrals inside the square brackets [...] contain the same term under the integration, that allows to rewrite the expression as:

$$\int_0^L ds \int_0^L dz \left[\int_0^s ds_2 \int_0^{s_2} ds_1 (s_2 - s_1) + \int_s^L ds_2 \int_0^s ds_1 (s_2 - s_1) + \int_s^L ds_2 \int_s^{s_2} ds_1 (s_2 - s_1) \right] \left(s + z - \frac{s^2}{L} \right)^{-\frac{d}{2}} \\ + \int_0^S ds \int_0^L dz \left[\int_0^s ds_2 \int_0^{s_2} ds_1 \left(-\frac{(s_2 - s_1)^2}{s + z - \frac{s^2}{L}} \right) + \int_s^L ds_2 \int_0^s ds_1 \left(-\frac{(s - s_1)^2}{s + z - \frac{s^2}{L}} \right) \right] \left(s + z - \frac{s^2}{L} \right)^{-\frac{d}{2}} \quad (35)$$

The last two terms in the first line can be joined since the limits of the integration over s_2 are the same and the integration over s_1 can be presented as one integral:

$$\int_0^S ds \int_0^L dz \left[\int_0^s ds_2 \int_0^{s_2} ds_1 (s_2 - s_1) + \int_s^L ds_2 \int_0^{s_2} ds_1 (s_2 - s_1) \right] \left(s + z - \frac{s^2}{L} \right)^{-\frac{d}{2}} + \\ \int_0^S ds \int_0^L dz \left[\int_0^s ds_2 \int_0^{s_2} ds_1 \left(-\frac{(s_2 - s_1)^2}{s + z - \frac{s^2}{L}} \right) + \int_s^L ds_2 \int_0^s ds_1 \left(-\frac{(s - s_1)^2}{s + z - \frac{s^2}{L}} \right) \right] \left(s + z - \frac{s^2}{L} \right)^{-\frac{d}{2}} \quad (36)$$

The similar arguments now may be presented for the case of integration over s_2 , so the final expression reads:

$$\int_0^S ds \int_0^L dz \left(s + z - \frac{s^2}{L} \right)^{-\frac{d}{2}} \left[\int_0^L ds_2 \int_0^{s_2} ds_1 (s_2 - s_1) \right] \\ + \int_0^S ds \int_0^L dz \left[\int_0^s ds_2 \int_0^{s_2} ds_1 \left(-\frac{(s_2 - s_1)^2}{s + z - \frac{s^2}{L}} \right) + \int_s^L ds_2 \int_0^s ds_1 \left(-\frac{(s - s_1)^2}{s + z - \frac{s^2}{L}} \right) \right] \left(s + z - \frac{s^2}{L} \right)^{-\frac{d}{2}} \quad (37)$$

Here the first term is reducible. The more interesting part is that in the first order of the perturbation theory only the diagrams that correspond to excluded volume interactions between points on the same trajectory (Diagrams 1 – 8, 12, 13, 20, 21, 23 – 26, 39 – 42, 44, 45) contain poles in their *epsilon*-expansions, that are not canceled by the partition sum. These diagrams are also easy to calculate. So for the rest of the diagrams we can make the calculations for either $d = 4$ or $d = 3$ and by taking into account only the terms that are not canceled. This way it is easier to handle the calculations also even in this simplification an expression for the *epsilon*-expansion will still contain the integral expressions that have to be handled numerically. Results for $d = 3$ are a bit more straightforward and thus are provided in the main part. As an example we present here the expressions for the radius of gyration of a dumbbell backbone for both $d = 3$ and *epsilon*-expansion:

$$\langle r_g^2 \rangle_{backbone}(d = 3) = \frac{3lL}{6} \left(1 - u_0 \left(-\frac{67}{315} - \frac{\pi(4l+1)}{24} + \frac{1}{12}(1/12) \arcsin \left((4l+1)^{-\frac{1}{2}} \right) (4l+1) \right. \right. \\ \left. \left. - \frac{\sqrt{l}(176l^4 - 128l^3 - 328l^2 - 130l - 15)}{90(1+2l)(4l+1)} - \frac{2l^4 \arctan \left(\frac{4l+1+\sqrt{2+4l}}{2\sqrt{l}} \right) - \arctan \left(\frac{4l+1-\sqrt{2+4l}}{2\sqrt{l}} \right)}{9(1+2l)\sqrt{2+4l}} \right) \right) \quad (38)$$

$$\langle r_g^2 \rangle_{backbone}(d = 4 - \epsilon) = \frac{dlL}{6} \left(1 - u_0 \left(-\frac{2}{\epsilon} + \frac{13}{12} - \ln(l) + 12l \int_0^1 \frac{\operatorname{arctanh} \left((1 - 4z^2 + 4l + 4z)^{-\frac{1}{2}} \right)}{(1 - 4z^2 + 4l + 4z)^{\frac{5}{2}}} dz \right. \right. \\ \left. \left. - \frac{l \operatorname{arctanh} \left(2 + 4l \right)^{-\frac{1}{2}} (8l + 7)}{\sqrt{2+4l}(1+2l)} + \frac{4l \operatorname{arctanh} \left((4l+1)^{-\frac{1}{2}} \right) (4l+3)}{(4l+1)^{\frac{3}{2}}} - \frac{(l-1)}{(1+2l)(4l+1)} \right. \right. \\ \left. \left. - \frac{2 \ln(2)(10l+3)}{5l^3} - \frac{1 \ln(4l+1)(40l^2 - 22l - 3)}{5l^3(4l+1)} - \frac{1}{150} \frac{1650l^3 + 250l^2 - 614l - 141}{l^3(4l+1)} \right. \right. \\ \left. \left. - \frac{3}{16l^3} \int_0^1 \frac{\ln \left(\frac{4l-x+1}{4l+1} \right) (-2(8l+3)(4l+1)^2 + 4(4l+1)(8l^2 + 12l + 3)x - (112l^2 + 96l + 18)x^2)}{\sqrt{x}(4l-x+1)^2} dx \right. \right. \\ \left. \left. - \frac{3}{16l^3} \int_0^1 \frac{\ln \left(\frac{4l-x+1}{4l+1} \right) ((32l+12)x^3 - 3x^4)}{\sqrt{x}(4l-x+1)^2} dx \right) \right) \quad (39)$$

-
- [1] Jacques Roovers. Viscoelastic properties of polybutadiene rings. *Macromolecules*, 21(5):1517–1521, 1988.
 - [2] T. McLeish. Chemistry. polymers without beginning or end. *Science*, 297(5589):2005–2006, 2002.
 - [3] Bertrand Duplantier. Statistical mechanics of polymer networks of any topology. *Journal of Statistical Physics*, 54(3-4):581–680, feb 1989.
 - [4] Walter Fiers and Robert L. Sinsheimer. The structure of the dna of bacteriophage ϕ x174: Iii. ultracentrifugal evidence for a ring structure. *Journal of Molecular Biology*, 5(4):424–434, 1962.
 - [5] Huan-Xiang Zhou. Effect of catenation on protein folding stability. *Journal of the American Chemical Society*, 125(31):9280–9281, 2003. PMID: 12889942.
 - [6] Bruno H. Zimm and Walter H. Stockmayer. The dimensions of chain molecules containing branches and rings. *The Journal of Chemical Physics*, 17(12):1301–1314, dec 1949.
 - [7] Jack Douglas and Karl F. Freed. Renormalization and the two-parameter theory. *Macromolecules*, 17(11):2344–2354, November 1984.
 - [8] Yuya Doi, Kazuki Matsubara, Yutaka Ohta, Tomohiro Nakano, Daisuke Kawaguchi, Yoshiaki Takahashi, Atsushi Takano, and Yushu Matsushita. Melt rheology of ring polystyrenes with ultrahigh purity. *Macromolecules*, 48(9):3140–3147, 2015.
 - [9] Jonathan D. Halverson, Gary S. Grest, Alexander Y. Grosberg, and Kurt Kremer. Rheology of ring polymer melts: From linear contaminants to ring-linear blends. *Phys. Rev. Lett.*, 108:038301, Jan 2012.
 - [10] Angelo Rosa, Jan Smrek, Matthew S. Turner, and Davide Michieletto. Threading-induced dynamical transition in tadpole-shaped polymers. *ACS Macro Letters*, 9(5):743–748, 2020. PMID: 33828901.
 - [11] Evelyne van Ruymbeke, Michael Kapnistos, Dimitris Vlassopoulos, Tianzi Huang, and Daniel M. Knauss. Linear melt rheology of pom-pom polystyrenes with unentangled branches. *Macromolecules*, 40(5):1713–1719, March 2007.
 - [12] T. C. B. McLeish and R. G. Larson. Molecular constitutive equations for a class of branched polymers: The pom-pom polymer. *Journal of Rheology*, 42(1):81–110, January 1998.
 - [13] R. S. Graham, T. C. B. McLeish, and O. G. Harlen. Using the pom-pom equations to analyze polymer melts in exponential shear. *Journal of Rheology*, 45(1):275–290, January 2001.
 - [14] Yuya Doi, Atsushi Takano, Yoshiaki Takahashi, and Yushu Matsushita. Viscoelastic properties of dumbbell-shaped polystyrenes in bulk and solution. *Macromolecules*, 54(3):1366–1374, 2021.

- [15] TX) Kiovsky, Thomas E. (Houston. Star-shaped dispersant viscosity index improver, March 1978.
- [16] Dimitris Vlassopoulos, Rossana Pasquino, and Frank Snijkers. *PROGRESS IN THE RHEOLOGY OF CYCLIC POLYMERS*, pages 291–316. WORLD SCIENTIFIC, 2013.
- [17] Guy C. Berry. An approximation for the intrinsic viscosity of brush-shaped polymers. *International Journal of Polymer Analysis and Characterization*, 12(4):273–284, 2007.
- [18] Chong Meng Kok and Alfred Rudin. Relationship between the hydrodynamic radius and the radius of gyration of a polymer in solution. *Makromol., Chem., Rapid Commun.*, 2(11):655–659, 1981.
- [19] Walther Burchard. *Solution Properties of Branched Macromolecules*, pages 113–194. Springer Berlin Heidelberg, Berlin, Heidelberg, 1999.
- [20] J.A. Aronovitz and D.R. Nelson. Universal features of polymer shapes. *Journal de Physique*, 47(9):1445–1456, 1986.
- [21] Zhi-Chao Yan, Md. D. Hossain, Michael J. Monteiro, and Dimitris Vlassopoulos. Viscoelastic properties of unentangled multicyclic polystyrenes. *Polymers*, 10(9), 2018.
- [22] Yasuyuki Tezuka. *Topological Polymer Chemistry*. WORLD SCIENTIFIC, 2013.
- [23] Hideaki Oike, Hiroyuki Imaizumi, Takayuki Mouri, Yuka Yoshioka, Akiko Uchibori, and Yasuyuki Tezuka. Designing unusual polymer topologies by electrostatic self-assembly and covalent fixation. *Journal of the American Chemical Society*, 122(40):9592–9599, 2000.
- [24] S F Edwards. The statistical mechanics of polymers with excluded volume. *Proceedings of the Physical Society*, 85(4):613, 1965.
- [25] Jaques des Cloizeaux and Gerard Jannink. *Polymers in Solution: their modelling and structure*. Clarendon Press:Oxford, 1991.
- [26] Marc L. Mansfield and Jack F. Douglas. Properties of knotted ring polymers. ii. transport properties. *The Journal of Chemical Physics*, 133(4):044904, 2010.
- [27] Yacov Kantor. Knots in polymers. *Pramana – Journal of Physics*, 64:1011–1017, june 2005.
- [28] E. Orlandini and S. G. Whittington. Statistical topology of closed curves: Some applications in polymer physics. *Rev. Mod. Phys.*, 79:611–642, Apr 2007.
- [29] Yoshitsugu Oono. *Statistical Physics of Polymer Solutions: Conformation-Space Renormalization-Group Approach*, pages 301–437. John Wiley and Sons, Ltd, 1985.
- [30] Gary S. Grest, Kurt Kremer, and T. A. Witten. Structure of many arm star polymers: a molecular dynamics simulation. *Macromolecules*, 20(6):1376–1383, nov 1987.
- [31] Gary S. Grest and Kurt Kremer. Molecular dynamics simulation for polymers in the presence of a heat bath. *Phys. Rev. A*, 33:3628–3631, May 1986.
- [32] Steve Plimpton. Fast parallel algorithms for short-range molecular dynamics. *Journal of Computational Physics*, 117(1):1–19, 1995.
- [33] Neal Madras and Alan D. Sokal. The pivot algorithm: A highly efficient monte carlo method for the self-avoiding walk. *J. Stat. Phys.*, 50(1-2):109–186, January 1988.
- [34] K. Haydukivska, O. Kalyuzhnyi, V. Blavatska, and Ja. Ilnytskyi. Swelling of asymmetric pom-pom polymers in dilute solutions. *Condensed Matter Physics*, 25:23302, 2022.
- [35] Nathan Clisby. Efficient implementation of the pivot algorithm for self-avoiding walks. *J. Stat. Phys.*, 140(2):349–392, May 2010.
- [36] Gaoyuan Wei. New approaches to shapes of arbitrary random walks. *Physica A: Statistical Mechanics and its Applications*, 222(1):155–160, 1995.
- [37] Christian von Ferber, Marvin Bishop, Thomas Forzaglia, Cooper Reid, and Gregory Zajac. The shapes of simple three and four junction comb polymers. *The Journal of Chemical Physics*, 142(2):024901, January 2015.
- [38] K. Haydukivska, O. Kalyuzhnyi, V. Blavatska, and Ja. Ilnytskyi. On the swelling properties of pom-pom polymers in dilute solutions. part 1: Symmetric case. *Journal of Molecular Liquids*, 328:115456, April 2021.
- [39] Khristine Haydukivska, Viktoria Blavatska, Jarosław S. Klos, and Jarosław Paturej. Conformational properties of hybrid star-shaped polymers comprised of linear and ring arms. *Phys. Rev. E*, 105:034502, Mar 2022.
- [40] Khristine Haydukivska, Viktoria Blavatska, and Jarosław Paturej. Universal size ratios of gaussian polymers with complex architecture: radius of gyration vs hydrodynamic radius. *Scientific Reports*, 10(1):2045–2322, August 2020.
- [41] K. Haydukivska and Blavatska. On the swelling properties of pom-pom polymers: impact of backbone length. *Condensed Matter Physics*, 26, 2023.
- [42] George Gaspari, Rudnick Joseph, and Arezki Beldjenna. The shapes of open and closed random walks: a l/d expansion. *J. Phys. A: Math. Gen.*, 20(11):3393, 1987.
- [43] O. Jagodzinski, E. Eisenriegler, and K. Kremer. Universal shape properties of open and closed polymer chains: renormalization group analysis and monte carlo experiments. *J. Phys. I France*, 2(12):2243–2279, 1992.